Vol. 24(3):197-205 | Ocean and Polar Research | September 2002

Article

Total Field Magnetic Analysis of Nine Seamounts Northwest of the Marshall Islands, Western Pacific

Tae-Gook Lee*[1], Sang-Mook Lee[1], Jae-Woon Moon[1], and Kiehwa Lee[2]

[1]*Marine Resources Laboratory, KORDI*
Ansan P.O. Box 29, Seoul 425-600, Korea
[2]*Department of Earth System Sciences, Seoul National University*
San 56-1, Shilim-dong, Kwanak-gu, Seoul 151-742, Korea

Abstract : Total magnetic field and high-resolution bathymetric data were collected over nine seamounts to the northwest of the Marshall Islands in the western Pacific. Magnetic parameters including inclination and declination were calculated from the magnetic anomalies using inversion algorithm of Plouff (1976), and a corresponding paleomagnetic pole was determined with the magnetic parameters. The paleomagnetic poles determined in this study were compared with the previous apparent polar wander path (APWP) of Pacific plate. Most seamounts of the study area have normal polarity. The study reveals that all nine seamounts in the study area formed in the southern hemisphere during the Cretaceous based on their comparison with the APWP of Pacific plate. The ages estimated from paleomagnetic poles can be divided by age into three groups: the oldest (OSM1 and OSM3), middle age (OSM2, OSM4, and 6-2), and the youngest (OSM5-1, 5-2, 5-3, and 6-1). The former two groups and the latter seem to be coincident with two distinct pulses of Cretaceous volcanic activity (115-90 Ma and 83-65 Ma). As a whole the seamounts at southwest of the study area are older than at those northeast.

Key words : total magnetic field, magnetic anomalies, apparent polar wander path, paleomagnetic poles.

1. Introduction

A characteristic feature of the western Pacific is the ubiquity of seamounts. Many of these seamounts in the western Pacific were created during the Cretaceous (65-145 Ma) when the volcanic activity was vigorous (Lincoln *et al.* 1993; van Waasbergen and Winterer 1993). One or two intervals in the Cretaceous are thought to have been specially energetic, where the production of intraplate volcanisms was widespread in the Pacific (Heezen *et al.* 1973d; Winterer 1976). Based on the analyses of samples collected by dredging and recovered by Deep Sea Drilling Project (DSDP) in the Line Islands and Nauru Basin (Schlanger and Premoli Silva 1981; Schlanger *et al.* 1981), the two distinct pulses of Cretaceous volcanic activity in the Central Pacific lasted during 115-90 Ma and 83-65 Ma. Rea and Vallier (1983) found a similar result from stratigraphic distribution of volcanogenic sediments from DSDP cores.

Methods for determining the age of seamount can be divided into direct and indirect methods in general. Radiometric dating from dredged samples is a good example of direct method (Koppers *et al.* 1998). Such direct method, though powerful, can be seriously affected by the degree of freshness of the sample rock and even if the sample is fresh, it is unclear whether the estimated age can be taken as representative age of the whole seamount. To overcome such difficulties, an indirect method based on paleomagnetism is often used (Sager 1983). The method calculates magnetic parameters from observed magnetic anomaly and estimates paleomagnetic pole corresponding to the anomaly. A good example of this method is Gordon (1983) and Sager (1983) who estimated the apparent polar wander path (APWP) of Pacific plate from the distribution

*Corresponding author. E-mail : tglee@kordi.re.kr

of seamount paleomagnetic poles. The advantage of this method is that one can obtain many data efficiently within limited survey time and minimize outliers through smoothing process, but its disadvantage is that there is no unique solution as is often the case for potential field method and that the results are highly dependent on the assumptions made in the model.

The aim of this study is to determine the paleopole and the age of seamounts using a paleomagnetic pole determined by Plouff's method and to find out whether seamounts in the study area were produced by the widespread intraplate volcanism in the Cretaceous.

Total magnetic field measurements were performed over nine seamounts to the northwest of the Marshall Islands in the western Pacific during manganese crust survey in June, 2000 and 2001 aboard the R/V *Onnuri*. These seamounts have not been mapped in detail and are not named except for two. They are denoted sequentially from southwest to northeast as open-sea seamount (OSM) and numbered as 1, 2, 3, 4, 5-1, 5-2, 5-3, 6-1, and 6-2 in this study. OSM1 and OSM5-2 corresponds to previously studied seamounts named Ita Mai Tai and Seascan guyot, respectively (Sager 1983; Heezen *et al.* 1973b). During our cruise, high-resolution multibeam bathymetric data were collected by SeaBeam 2000. Total magnetic field were collected by proton precession magnetometer towed 200 m behind the ship near the sea surface not to be affected by the magnetic effect from ship. In addition, multichannel seismic profiles and 3.5 kHz sub-bottom profiles were obtained over each seamount.

2. Tectonic settings

The study area is located between Pigafetta basin and East Mariana basin (Fig. 1). It is bounded to the west by the Mariana Trench, to the southwest by the Caroline Islands, and to the southeast by the Marshall Islands. OSM1, 3 and 2, 4 are located on southeastern border of Magellan Seamount Trail (MST) and OSM5 and 6 on its northeastern border (Fig. 2)(according to Smith *et al.* 1989). Kopper *et al.* (1998) estimated that the age of three MST seamounts northwest of OSM1 is between 87 and 95 Ma. Ogasawara fracture zone (OFZ) #1 runs between OSM1, 2, 3 and 4 and divides the seamounts into two area (Figs. 1 and 2)(Kopper *et al.* 1997). The study area is far from well defined magnetic anomaly lineations (Nakanishi and Winterer 1998). However, the age of seafloor in the southwest corner, is inferred to be as old as Middle

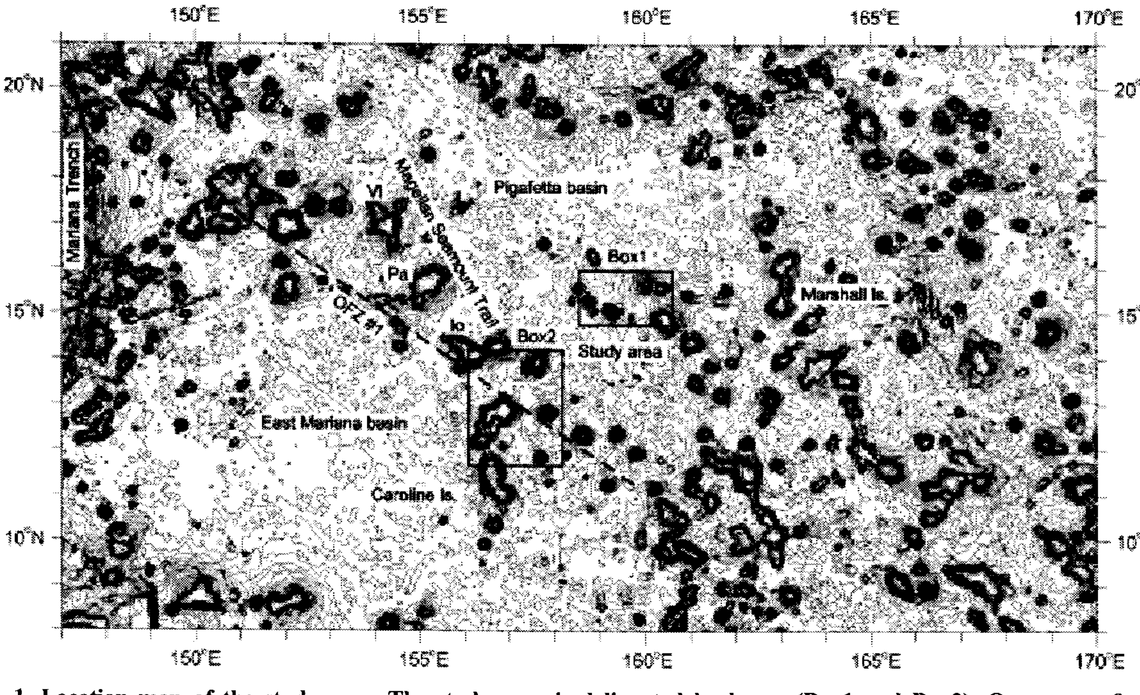

Fig. 1. Location map of the study area. The study area is delineated by boxes (Box1 and Box2). Ogasawara fracture zone (OFZ) #1 is a dotted line based on Koppers *et al.* (1997). In Magellan Seamount Trail (MST), Vlinder (95.1 Ma) is abbreviated as Vl, Pako (91.3 Ma) as Pa, and Ioah (87.1 Ma) as Io (Koppers *et al.* 1998).

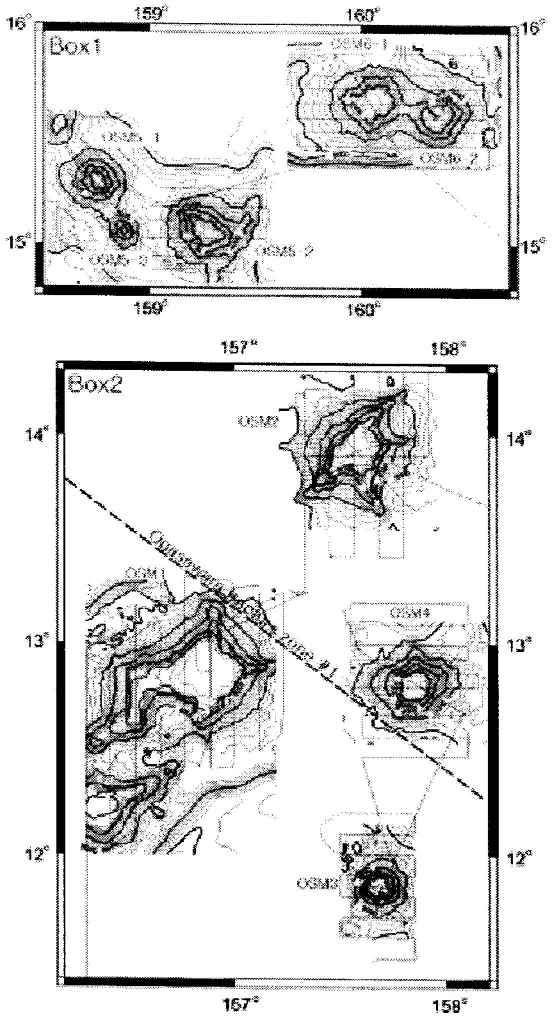

Fig. 2. Bathymetric map of Box 1 and Box 2 in Fig. 1 showing seamounts OSM1-6. Thin solid lines are ship tracks. Contour interval is 200 m.

Jurassic (161-174 Ma) (Tamaki *et al.* 1987; Nakanishi *et al.* 1989). From two rock samples recovered on the northeast slope of Ita Mai Tai, Koppers *et al.* (1998) dated 118 Ma as their age. One hole (DSDP Site 199) was drilled on northwest of Ita Mai Tai at 13° 31'N, 156° 10'E and three holes (DSDP Sites 200, 201 and 202) on the summit of Ita Mai Tai at 12° 45'N, 156° 45'E (Heezen *et al.* 1973a, b, c).

3. Bathymetry

The bathymetry and survey track lines are shown in Fig. 2. Seven seamounts except OSM5-1 and OSM5-3 are guyot with flat summit. On a plan view, most seamounts in the study area are spindle-shaped, but OSM1 is L-shaped and OSM6-2 V-shaped. OSM1 is connected with a small seamount to southwest. However, bathymetic survey did not fully cover this small seamount.

The depth of abyssal plain of the study area ranges from 5,200 m near OSM6 to 6,000 m near OSM1. It becomes shallower from southwest to northeast (Fig. 1 and Table 1). The summit of OSM6-1 at 1,100 m below the sea level is the shallowest, and the summit of OSM1 at 1,400 m is the deepest among seamounts (Fig. 2 and Table 1). OSM1 is the largest seamounts in the study area, and OSM5-3 is the smallest seamount with peaked summit.

Seamounts located to the south tend to have thicker pelagic sediments on their summits than those in the northern part (Table 1). OSM1 has the thickest pelagic cap with over 100-m-thick layer. OSM2, 3 and 4 have over 40 m of sediment. The pelagic caps of OSM5 and OSM6 are less than 20 m thick.

Table 1. Classification and description of seamounts of the study area by geomorphology, bathymetry and pelagic sediment.

	Type of seamount	Depth of summit (m)	Depth of base (m)	Diameter of base (km)		Pelagic cap* (m)	Pelagic sediment** (m)
				Major axis	Minor axis		
OSM1	Guyot	1400	6000	100	90	150	60
OSM2	Guyot	1300	6000	75	65	50	40
OSM3	Guyot	1300	6000	40	35	45	80
OSM4	Guyot	1300	6000	55	45	70	50
OSM5-1	Peaked seamount	1300	5400	40	35	0	35
OSM5-2	Guyot	1200	5400	55	45	15	15
OSM5-3	Peaked seamount	2400	5400	20	15	0	20
OSM6-1	Guyot	1100	5200	55	45	5	15
OSM6-2	Guyot	1200	5200	45	40	0	15

*Maximum thickness of pelagic cap at the summit calculated from Sub-bottom profile with constant velocity 1500 m/s.
**Maximum thickness of pelagic sediments at the base determined from Sub-bottom profile with seismic velocity 1500 m/s.

4. Method

Although most seamounts can be approximated to a simple magnetic model, some seamounts can have quite a complex magnetic structure and property. The method for inverting magnetization can only be successful when the magnetic structure is relatively simple. The following assumptions are made to make a simple model, and a measure is employed to quantify the match between the observed and modeled. The validity of these assumptions was discussed by Sager (1983).

(1) Magnetization is assumed to be homogeneous throughout the entire body of seamount.
(2) Magnetic anomaly is caused solely by thermoremanent magnetization.
(3) The bottom of the seamount is assumed to be flat.
(4) The seamount is thought to have formed over a sufficiently long interval of time such that secular variation can be averaged out.

The first three assumptions are necessary to make the model tractable. Most seamounts form at a relatively short time, and therefore the chance of having polarity reversals during the formation is quite small. However, if seamount formed in multi-stage and if there is a large time gap between the main and post-shield volcanism, the first assumption may not hold. In general, because igneous rocks comprise the bulk of seamount, the thermoremanent magnetization is the dominant component of magnetization. Due to the weight of seamount, the basement of crust can be flexed giving rise to curved basement. However, the amount of downwarping is generally less than few hundred meters in vertical scale. Therefore, deviation from flat basement can be neglected considering the lateral scale of the seamount. If the rocks of seamount record the geomagnetic field over a period of time long enough (usually 10^4-10^5 year), then the average field would be that of an axial geocentric dipole (Merrill *et al.* 1998).

Magnetic anomaly was obtained by subtracting the long wavelength region field, International Geomagnetic Reference Field (IGRF), from the total magnetic field data. Diurnal variations were removed from the magnetic field using the magnetic observation at Guam station (13.4°N, 144.7°E). With the method of Plouff (1976) the resulting magnetic anomaly data were inverted for best-fitting, least-squares, uniform magnetization.

Plouff's method is an improvement of the earlier method of Talwani (1965) that calculates the components of the magnetic anomalies caused by a finite homogeneously magnetized body of arbitrary shape. In a right-handed coordinate system for a volume element Δx, Δy, Δz within a body Q, the magnetic potential at the origin, Ω is given by

$$\Omega = \boldsymbol{u} \cdot \boldsymbol{R}/R^3 \tag{1}$$

where, $\boldsymbol{u}$ is the magnetic moment of the volume element and $\boldsymbol{R}$ the distance vector. If $\boldsymbol{J}$ is the uniform intensity of magnetization of Q, and then $\boldsymbol{u} = \boldsymbol{J} \cdot \Delta x \cdot \Delta y \cdot \Delta z$. The three components X, Y and Z of magnetic anomaly can be written as

$$\begin{aligned} X &= \iiint -\frac{\partial \Omega}{\partial x} dx\, dy\, dz = J_x V_1 + J_y V_2 + J_z V_3 \\ Y &= \iiint -\frac{\partial \Omega}{\partial y} dx\, dy\, dz = J_x V_2 + J_y V_4 + J_z V_5 \\ Z &= \iiint -\frac{\partial \Omega}{\partial z} dx\, dy\, dz = J_x V_3 + J_y V_5 + J_z V_6. \end{aligned} \tag{2}$$

$$\text{where, } V_1 = \iiint \frac{3x^2 - R^2}{R^5} dxdydz, \quad V_2 = \iiint \frac{3xy}{R^5} dxdydz,$$
$$V_3 = \iiint \frac{3xz}{R^5} dxdydz, \quad V_4 = \iiint \frac{3y^2 - R^2}{R^5} dxdydz,$$
$$V_5 = \iiint \frac{3yz}{R^5} dxdydz, \text{ and } V_6 = \iiint \frac{3z^2 - R^2}{R^5} dxdydz. \tag{3}$$

The $V_1 - V_6$ are volume integrals involving the dimensions of the seamount and its distance from the point of observation. To calculate the integration over volume in equation (3), the seamount is decomposed into polygonal prisms.

The total magnetic anomaly T at an observation point is given by

$$T = \sqrt{(lH + X)^2 + (mH + Y)^2 + (nH + Z)^2} - H \tag{4}$$

where, l, m, and n are the direction cosines of the Earth's field and H magnitude of the Earth's field. If the anomaly T is small compared to the main field H, then we can write equation (4) as follows

$$T \approx lX + mY + nZ \tag{5}$$

Substituting X, Y, and Z of equation (2) into formula (5), one finds

$$\begin{aligned} T &= J_x(lV_1 + mV_2 + nV_3) + J_y(lV_2 + mV_4 + nV_5) \\ &\quad + J_z(lV_3 + mV_5 + nV_6) \\ &= J_x B_1 + J_y B_2 + J_z B_3 \end{aligned} \tag{6}$$

where, B_1, B_2, and B_3 are the functions of seamount's volume using V calculated in equation (3). The total magnetization can be divided into two: that is, the induced magnetization and remanent magentization. To deduce paleomagnetic field direction when seamount erupted and formed, induced magnetic anomaly terms should be removed, in which case $J_x = J_r L$, $J_y = J_r M$, and $J_z = J_r N$. J_r is the intensity of remanent magnetization, and L, M, and N the direction cosines of the remanent magnetization vector. Equation (6) after removing the induced magnetization can be written as follows

$$T = J_r L B_1 + J_r M B_2 + J_r N B_3 \quad (7)$$

If T, B_1, B_2, and B_3 are known, then magnetic parameters J_r, L, M, and N can be calculated by the least square method.

In order to quantify the agreement between the field calculated and the observed anomaly, we used goodness-of-fit ratio (GFR) generally adopted in seamount inversions (Richards *et al.* 1967).

$$GFR = \sum_i |A_i| / \sum_i |E_i| \quad (8)$$

Here A_i is the sum of magnitudes of the observed magnetic anomaly and E_i the sum of magnitudes of the misfit between the magnetic anomaly calculated from the best-fit uniform magnetization and the observed magnetic anomaly. Generally, GFR less than 1.8 is considered as a bad match and can not be trusted (Harrison *et al.* 1975).

Given the present location (λ_s, ϕ_s) of seamount and the inclination $I_m (= \tan^{-1}(J_z / \sqrt{J_x^2 + J_y^2})$ and declination D_m $(= \tan^{-1}(J_y / J_x))$ calculated from above procedure, one can estimate the paleomagnetic pole location (λ_p, ϕ_p) (Merrill *et al.* 1998).

$$\sin\lambda_p = \sin\lambda_s \cdot \cos\theta + \cos\lambda_s \cdot \sin\theta \cdot \cos D_m \quad (-90^\circ \le \lambda_p \le +90^\circ)$$

$$\phi_p = \phi_s + \beta \quad (\cos\theta \ge \sin\lambda_s \cdot \sin\lambda_p)$$
$$\text{or } \phi_p = \phi_s + 180 - \beta \quad \cos\theta < \sin\lambda_s \cdot \sin\lambda_p \quad (9)$$

The paleocolatitude θ is $\cot^{-1}(0.5 \cdot \tan I_m)$ and β is $\sin^{-1}(\sin\theta \cdot \sin D_m / \cos\lambda_p)$.

To represent the confidence on the paleomagnetic pole estimation of the seamounts, we used an oval of 95% confidence for the paleomagnetic pole. A circle of 95% confidence (α_{95}) for directions of the magnetization vector is transformed to an oval of 95% confidence ($\delta\theta$, δ_m) for the paleomagnetic pole. A circular cone of semi-angle α_{95} is same as the error ΔI in inclination (Irving 1956). The parameter $\delta\theta$ $(= 0.5\alpha_{95}(1 + 3\cos^2\theta))$ is the uncertainty in the paleocolatitude, and δm $(= \alpha_{95} \sin\theta / \cos I)$ is the uncertainty in direction perpendicular to the paleomeridian of the paleopole (Merill *et al.* 1998).

5. Results and discussion

The results of the magnetic inversions calculated in this study are summarized in Table 2 and Figs. 3, 4, and 5. OSM1 exhibits a pair of small positive and negative anomalies next to a large one (Fig. 3). Because we are interested in the overall distribution magnetic anomaly, such small local anomalies are ignored at this time. All seamounts in the study area except OSM3 are normally polarized. Therefore most of the seamounts have negative peak anomaly in the central and positive anomalies to the north and south. The northern anomaly peak is higher

Table 2. Seamount paleomagnetic parameters.

	Location		Paleopole		α_{95}* (°)	Paleolatitude $90° - \theta$ (°S)	GFR**	Inclination I_m (+Down)	Declination D_m (+East)	Magnetic intensity J_r (A/m)
	Latitude ϕ_s (°N)	Longitude λ_s (°E)	Latitude ϕ_p (°N)	Lonitude λ_p (°E)						
OSM1	12.9	156.9	37.6	310.6	2.0	33.8	2.3	−53.2	25.0	2.7
OSM2	13.9	157.6	59.5	312.1	1.7	13.8	2.2	−26.1	13.0	6.8
OSM3	11.8	157.7	30.8***	258.2***	3.5	21.4	2.5	38.1	−130.2	0.2
OSM4	12.8	157.9	57.9	319.3	0.5	17.7	6.6	−32.5	10.2	5.0
OSM5-1	15.3	158.8	64.1	335.6	1.1	10.5	4.6	−20.4	1.4	3.0
OSM5-2	15.1	159.3	49.6	4.4	0.5	21.7	4.6	−38.5	−17.2	8.7
OSM5-3	15.1	158.9	52.9	359.0	1.4	19.8	9.1	−35.8	−12.7	2.2
OSM6-1	15.7	160.1	56.9	342.7	0.7	17.4	4.2	−32.1	−1.5	9.0
OSM6-2	15.6	160.4	56.3	325.3	1.2	17.0	5.3	−31.5	8.7	6.2

*α_{95} is the radius of the circle of 95% confidence about the mean.
**GFR is a goodness-of-fit ratio.
***South pole for seamounts with reversed polarity.

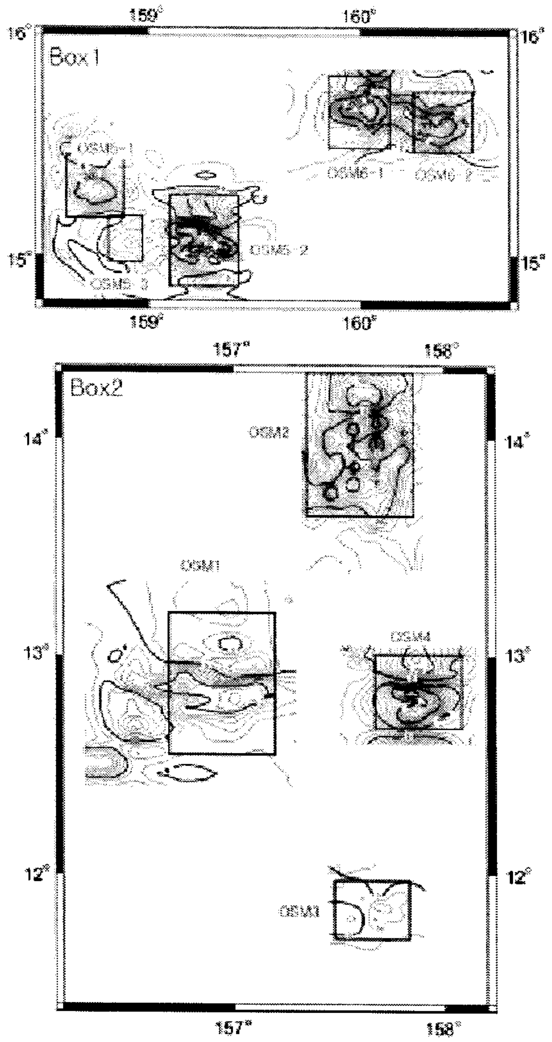

Fig. 3. **Observed magnetic anomalies of the study area. Contour interval is 50 nT. Thick solid contour is 300 nT interval. The anomaly of OSM3 exhibits narrow range of variation.**

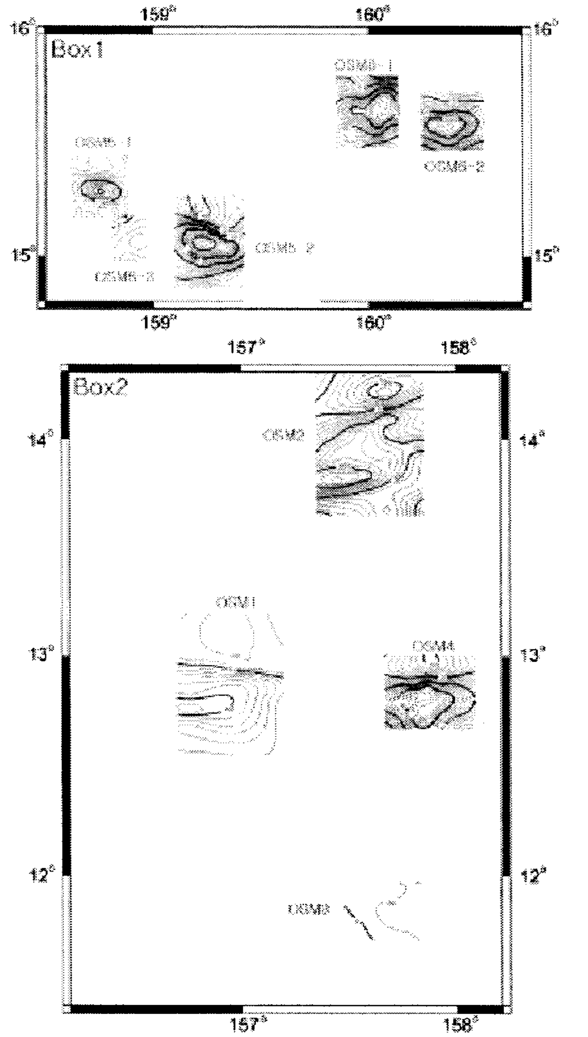

Fig. 4. **Calculated magnetic anomalies of the study area. Contour interval is 50 nT. Thick solid contour is 300 nT interval.**

than the southern one. If seamount formed near the equator with normal polarity, negative peak anomaly should appear in the center of seamount with positive anomalies to the north and south. The north positive peak should increase in magnitude as the seamount formed further south from the equator. Therefore, the seamounts of the study area appear to have formed below the equator and moved northward with the motion of Pacific plate. In case of OSM3, the peak anomalies trend almost east-west (Fig. 3). If we assume Earth as a geocentric axial dipole, the magnetization direction of seamount would be north-south. Since OSM3 is at least 100 km away from the nearest seamount, it could not be the effect of the neighboring seamount. This apparent misalignment suggests either that OSM3 has rotated after the formation or that intrusion at the west of OSM3 occurred without making any mount.

The GFR of seamounts in the study area is moderate to high and ranges from 2.2 to 9.1, which suggests that the calculated anomaly has a good correlation with the observed anomaly (Table 2). OSM1, 2 and 3 have low GFR, while OSM5-3 has a very high GFR, while OSM1 and OSM2 are very large in size, and OSM5-3 is very small. Our results are consistent with the findings of Sager (1983) that the smaller the size of seamount or observed anomaly is, the higher the GFR is.

Using the present location of seamount, inclination and

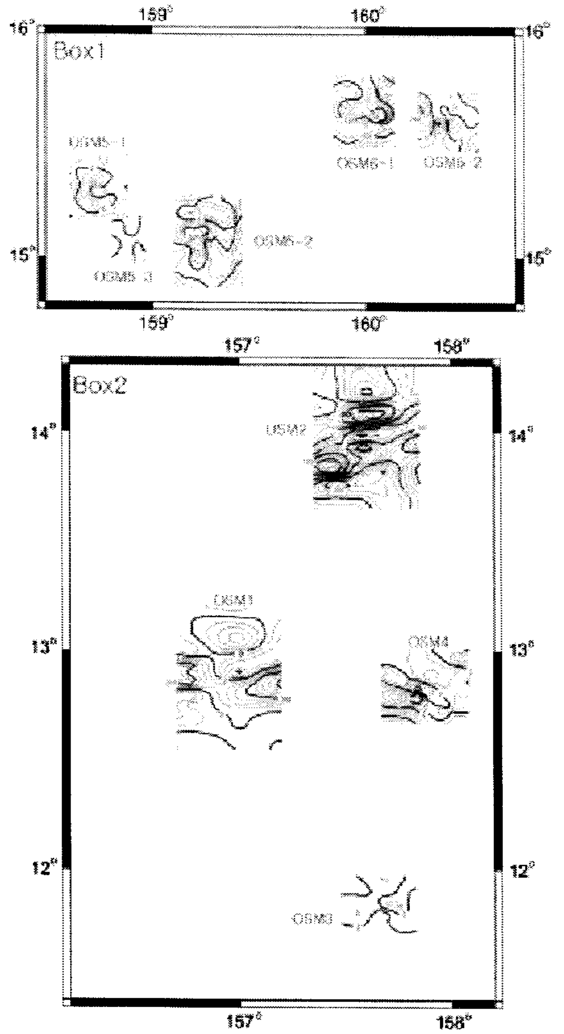

Fig. 5. Residual magnetic anomalies of the study area. Contour interval is 50 nT. Thick solid contour is 200 nT interval.

declination calculated from magnetic inversion, we calculated the paleopoles of seamounts. Figure 6 shows the poles in comparison with the Pacific APWP as determined by Sager (1983), Sager and Pringle (1988), and Tarduno and Sager (1995). The mean paleopole positions of the seamounts are shown as dotted ellipses and poles for the Pacific APWP are indicated as solid ellipses with ages in Ma (Fig. 6). Most paleopoles of seamounts in the study area show a good agreement with the APWP of Pacific plate.

The paleopole of OSM3, however, is far from the APWP of Pacific plate. Even though calculated without magnetic anomaly at the west slope of OSM3, paleomagnetic pole (74°E, 40°N) deviated far from the APWP of Pacific plate.

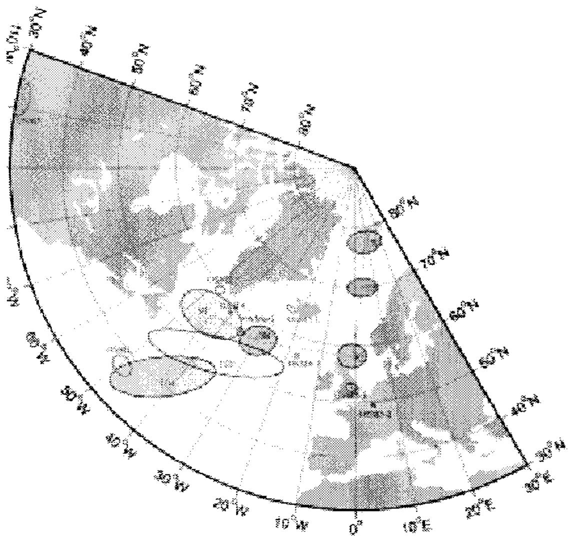

Fig. 6. Apparent Polar Wander Path (APWP) of the Pacific plate (dashed line) and seamount paleopoles determined from this study. Solid circles with numbers are poles for the Pacific APWP with 95% confidence and dotted circles are the mean paleopole positions of seamounts with 95% confidence. APW of 91 and 104 Ma are from Sager (1983), APWP of 39, 72, 82, and 88 Ma from Sager and Pringle (1988), and APWP of 129 Ma from Tarduno and Sager (1995).

Under the condition that OSM3 rotated, when the declination is set to that of OSM1, the paleopole is located between 104 and 91 Ma as 58.9°W, 48.6°N. The paleopole of OSM1 lies near 104-Ma pole of Pacific APWP determined by Sager (1983) which is different from its radiometric dating. It is possible that OSM1 first erupted during the early Cretaceous and since then it experienced post-shield eruption (Wedgeworth and Kellogg 1987; Lee *et al.* 2001). OSM1 and OSM3, south of the OFZ #1, seem to align with the MST (Fig. 1). OSM1 and OSM3 do not show age progression consistent with a single hotspot model. Paleopoles of OSM2 and OSM4 are close to 91-Ma Pacific APWP of Sager (1983). Although the location of OSM5-3 is closer to OSM5-1 than OSM5-2 in distance and similar to OSM5-1 in morphology, the paleopole of OSM5-3 is closer to that of OSM5-2. The paleopole of OSM5-1 is close to 88-Ma pole of Pacific APWP and those of OSM5-2 and OSM5-3 are close to 82-Ma pole. The gap between them may due to influence by the induced magnetic field and/or non-dipole magnetic Earth field. The paleopole of OSM6-1 lies between 88 and 82 Ma and that of OSM6-2 close to 91 and 88 Ma.

The ages estimated from paleomagnetic poles can be divided by age into three groups: the oldest (OSM1 and OSM3), middle age (OSM2, OSM4, and 6-2), and the youngest (OSM5-1, 5-2, 5-3, and 6-1). The former two groups and the latter seem to be coincident with two distinct pulses of Cretaceous volcanic activity (115-90 Ma and 83-65 Ma). There appears to be no age progression in the seamounts of the study area, but as a whole the seamounts at southwest of the study area are older than at those northeast.

According to our estimate of the paleolatitudes (Table 2), OSM4, 6-1 and 6-2 formed at similar latitude, while the group of seamounts consisting OSM3, 5-2 and 5-3 formed at another latitude. The age estimated from the paleomagnetic pole and the paleolatitude of the seamounts do not appear to be consistent. The induced magnetic field and/or non-dipole magnetic field made by the secular variation may affect the uncertainty of the paleomagnetic pole. If seamounts erupted at one region and Pacific plate has moved northward, the higher the latitude of the seamount is, the older the seamount should be. However, Pacific plate motion between 129 Ma and 91 Ma is rather uncertain, it is unclear if the seamounts formed simultaneously.

6. Conclusions

1. The seamounts in the study area can be divided into two groups on the basis of depth of base, thickness of pelagic cap, and thickness of pelagic sediments at the base. The first group (OSM1, 2, 3 and 4) is generally at the base and has thicker pelagic sediments that the second group (OSM 5 and 6).

2. The seamounts in the study area can be divided into three groups on the basis of their paleomagnetic ages compared with the Pacific APWP: the oldest (OSM1 and OSM3), middle age (OSM2, OSM4, and 6-2), and the youngest (OSM5-1, 5-2, 5-3, and 6-1). The former two groups and the latter seem to be coincident with two distinct pulses of Cretaceous volcanic activity (115-90 Ma and 83-65 Ma).

3. Most seamounts of the study area have normal polarity except OSM3. The peak anomalies of OSM3 should east-west trend, which suggests either that it has rotated since formation or that intrusion at the west of it occurred without making any mount.

4. All seamounts in the study area were formed in the southern hemisphere and OSM1, OSM3 and Magellan seamounts seem to lie in the path predicted by plate rotation model, but the paleomagnetic ages do not follow an age progression consistent with the single hotspot model.

5. Paleolatitudes calculated from inclination of seamount show that they can be divided into two groups by their formation latitude. OSM4, 6-1, and 6-2 belong to one group and OSM3, OSM5-2 and 5-3 belong to the other. However, because Pacific plate motion between 129 Ma and 91 Ma is poorly constrained, there is a large uncertainty associated with this argument and it is difficult to tell whether the seamounts formed simultaneously or not.

Acknowledgements

The authors thank researchers and crew members of R/V *Onnuri* who help to obtain and process data. Thanks are extended to Drs. Young-Keun Jin and Dongwoo Suk for their constructive comments to this manuscript. This study is supported by the Ministry of Maritime Affairs and Fisheries of Korea.

References

Gordon, R.G. 1983. Late Cretaceous apparent polar wander path of the Pacific plate: Evidence of a rapid shift of the Pacific hotspots with respect to the paleomagnetic axis. *Geophys. Res. Lett.*, 10, 709-712.

Harrison, C.G.A., R.D. Jarrard, V. Vacquier, and R.L. Larson. 1975. Paleomagnetism of Cretaceous Pacific seamounts. *Geophys. J. R. Astron. Soc.*, 42, 859-882.

Heezen B.C., I.D. MacGregor, H.P. Foreman, G. Forristall, H. Hekel, R. Hesse, R.H. Hoskins, E.J.W. Jones, A. Kaneps, V.A. Krasheninnikov, H. Okada, and M.H. Ruef. 1973a. Mesozoic chalks beneath the Caroline abyssal plain: DSDP Site 199. *Initial Rep. Deep Sea Drill. Proj.*, 20, 65-86.

Heezen, B.C., I.D. MacGregor, H.P. Foreman, G. Forristall, H. Hekel, R. Hesse, R.H. Hoskins, E.J.W. Jones, A. Kaneps, V.A. Krasheninnikov, H. Okada, and M.H. Ruef. 1973b. Tertiary pelagic ooze on Ita Maitai guyot, equatorial Pacific DSDP Sites 200 and 201. *Initial Rep. Deep Sea Drill. Proj.*, 20, 87-96.

Heezen, B.C., I.D. MacGregor, H.P. Foreman, G. Forristall, H. Hekel, R. Hesse, R.H. Hoskins, E.J.W. Jones, A. Kaneps, V.A. Krasheninnikov, H. Okada, and M.H. Ruef. 1973c. Oolitic limestone on the Ita Maitai guyot, Equatorial Pacific: DSDP Site 202. *Initial Rep. Deep Sea Drill. Proj.*, 20, 97-102.

Heezen, B.C., J.L. Matthews, R. Catalano, J. Natland, A. Coogan, M. Tharp, and M. Rawson. 1973d. Western Pacific guyots. *Initial Rep. Deep Sea Drill. Proj.*, 20, 653-723.

Irving, E. 1956. Paleomagnetic and paleoclimatological aspects of polar wandering. *Geofis. Pura. Appl.*, 33, 23-41.

Koppers, A.A.P., H. Staudigel, J.R. Wijbrans, and M.S. Pringle. 1998. The Magellan seamount trail: Implications for Cretaceous hotspot volcanism and absolute Pacific plate motion. *Earth Planet. Sci. Lett.*, 163, 53-68.

Lee, T.G., S.M. Lee, and J.W. Moon. 2001. Magnetic anomaly analysis of two adjacent seamounts (Ita Mai Tai and OSM2) in the western Pacific. *J. Geol. Soc. Korea*, 37, 587-596.

Lincoln, J.M., M.S. Pringle, and I.P. Silva. 1993. Early and Late Cretaceous Volcanism and Reef-Building in the Marshall Islands. p. 279-305. In: *The Mesozoic Pacific: Geology, Tectonics, and Volcanism,* eds. by M.S. Pringle, W.W. Sager, W.V. Silter, and S. Stein. American Geophysical Union.

Merrill, R.T., M.W. EcElhinny, and P.L. McFadden. 1998. *The Magnetic Field of the Earth.* Academic Press, San Diego, 631 p.

Nakanishi, M., K. Tamaki, and K. Kobayashi. 1989. Mesozoic magnetic anomaly lineations and seafloor spreading history of the northwestern Pacific. *J. Geophys. Res.*, 94, 15437-15462.

Nakanishi, M. and E.L. Winterer. 1998. Tectonic history of the Pacific-Farallon-Phoenix triple junction from Late Jurassic to Early Cretaceous: An abandoned Mesozoic spreading system in the Central Pacific Basin. *J. Geohpys. Res.*, 103, B6, 12453-12468.

Plouff, D. 1976. Gravity and magnetic fields of polygonal prisms and application to magnetic terrain corrections. *Geophysics*, 41, 727-741.

Rea, D.K. and T.L. Vallier. 1983. Two Cretaceous volcanic episodes in the western Pacific Ocean. *Geol. Soc. Am. Bull.*, 94, 1430-1437.

Richards, M.L., V. Vacquier, and G.D. van Voorhis. 1967. Calculation of the magnetization of uplifts from combining topographic and magnetic surveys. *Geophysics*, 32, 678-707.

Sager, W.W. 1983. Seamount paleomagnetism and Pacific plate tectonics. Ph.D. Thesis, Univ. Hawaii. Honolulu. 472 p.

Sager, W.W. and M.S. Pringle. 1988. Mid-Cretaceous to early Tertiary apparent polar wander path of the Pacific plate. *J. Geophys. Res.*, 93, 11753-11771.

Schlanger, S.O., H.C. Jenkyns, and I. Premoli-Silva. 1981. Volcanism and vertical tectonics in the Pacific Basin related to global Cretaceous transgressions. *Earth Planet. Sci. Lett.*, 52, 435-449.

Schlanger, S.O. and I. Premoli-Silva. 1981. Tectonic, volcanic, and paleogeographic implications of redeposited reef faunas of Late Cretaceous and Tertiary age from the Nauru Basin and the Line Islands. *Initial Rep. Deep Sea Drill. Proj.*, 61, 817-827.

Smith, W.H.F., H. Staudigel, A.B. Watts, and M.S. Pringle. 1989. The Magellan Seamounts: Early Cretaceous Record of the South Pacific Isotopic and Thermal Anomaly. *J. Geophys. Res.*, 94, 10501-10523.

Talwani, M. 1965. Compuation with the help of a digital computer of magnetic anomalies caused by bodies of arbitrary shape. *Geophysics*, 30, 797-817.

Tamaki, K., K. Nakanishi, K. Sayanagi, and K. Kobayashi. 1987. Jurassic magnetic anomaly lineations of the Western Pacific and the origin of the Pacific plate. *EOS, Trans. AGU*, 68, 1493.

Tarduno, J.A. and W.W. Sager. 1995. Polar Standstill of the Mid-Cretaceous Pacific Plate and Its Geodynamic Implications. *Science*, 269, 956-959.

van Waasbergen, R.J. and E.L. Winterer. 1993. Summit Geomorphology of Western Pacific Guyots. p. 335-366. In: *The Mesozoic Pacific: Geology, Tectonics, and Volcanism,* eds. by M.S. Pringle, W.W. Sager, W.V. Silter, and S. Stein. American Geophysical Union.

Wedgeworth, B. and J. Kellogg. 1987. A 3-D gravity-tectonic study of Ita Mai Tai guyot: an uncompensated seamount in the East Mariana Basin. p. 25-34. In: *Seamounts, Islands and Atolls*, eds. by B.H. Keating, P. Fryer, R. Batiza, and G.W. Boehlen. American Geophysical Union.

Winterer, E.L. 1976. Bathymetry and regional tectonic setting of the Line Islands Chain. *Initial Rep. Deep Sea Drill. Proj.*, 33, 731-748.

Received May 1, 2002
Revised Jul. 10, 2002
Accepted Sep. 30, 2002